Applied Catalysis A: General 469 (2014) 398–409

Contents lists available at ScienceDirect

Applied Catalysis A: General

journal homepage: www.elsevier.com/locate/apcata

Influence of acid-base sites on ZnO–$ZnCr_2O_4$ catalyst during dehydrocyclization of aqueous glycerol and ethylenediamine for the synthesis of 2-methylpyrazine: Kinetic and mechanism studies

Akula Venugopal[a,*], Reema Sarkari[a], Chatla Anjaneyulu[a], Vankudoth Krishna[a], Mandari Kotesh Kumar[a], Nama Narender[a], Aytam Hari Padmasri[b]

[a] Catalysis Laboratory, Inorganic & Physical Chemistry Division, CSIR-Indian Institute of Chemical Technology (CSIR-IICT), Tarnaka, 500 607 Hyderabad, Andhra Pradesh, India
[b] Department of Chemistry, University College for Women, Osmania University, Koti, Hyderabad 500 095, Andhra Pradesh, India

ARTICLE INFO

Article history:
Received 26 July 2013
Received in revised form 10 October 2013
Accepted 13 October 2013
Available online 19 October 2013

Keywords:
2-Methylpyrazine
ZnO–$ZnCr_2O_4$
O_2 pulse chemisorption
NH_3–CO_2 TPD
Pyridine-2,6-dimethylpyridine FTIR

ABSTRACT

The physicochemical characteristics of ZnO–$ZnCr_2O_4$ (Zn–Cr–O) mixed oxides were determined by adsorption and spectroscopic methods. The catalytic activities of Zn–Cr–O was investigated for dehydrocyclization of ethylenediamine and aqueous glycerol to synthesize 2-methylpyrazine (2MP). Reductive pre-treatment was required for better 2MP yields and rate of 2MP was dependent upon strong basicity of Zn–Cr–O. Product distribution revealed that cyclocondensation of glycerol and ethylenediamine followed by homo-coupling of 2-pyrazinylmethanol occurred on moderate acid and strong base sites. On the contrary weak to moderate acidic and base sites were inefficient for homo-coupling of 2-pyrazinylmethanol. Role of acid-base properties was examined by pyridine and 2,6-dimethylpyridine poisoning studies.

1. Introduction

During the last two decades R&D was focussed on alternate fuels particularly the production of bio-diesel from bio-mass derived compounds. This has led to many challenges to the technologists from the view point of clean and economical manufacturing of bio-diesel as glycerol was found to be a greater concern by various aspects in order to commercialize the bio-diesel plants. Recovery and effective utilization of biodiesel co-products, such as glycerol, is one of the main options to be considered to lower the overall cost of biodiesel production. Several alternatives are being explored to make use of bio-glycerol to produce various commodity and fine chemicals [1,2]. Hence, utilization of such glycerol for the production of fine chemicals has been a topic of interest. 2-Methylpyrazine (2MP) is an intermediate compound for the synthesis of 2-amido pyrazine, a well-known bacteriostatic and antitubercular drug. 2MP is conventionally synthesized by using EDA and 1,2-propylene glycol over modified Zn–Cr–O catalysts [3]. In our previous work, dehydrocyclization activities and the 2MP rates were discussed based on surface acidities of the Zn–Cr–O catalysts [4].

In the present paper we extensively studied the influence of acid-base sites on Zn–Cr–O catalyst towards 2MP and 2-pyrazinylmethanol rates. The Zn–Cr–O activities are rationalized with poisoning studies using pyridine (Bronsted and Lewis acid site blocker) and 2,6-dimethylpyridine as a selective Bronsted acid site blocker in order to emphasize the role of surface acid-base sites on product distribution. A reaction mechanism during dehydrocyclization of EDA and bio-glycerol was established in conjunction with the physicochemical properties of Zn–Cr–O samples by using X-ray photoelectron spectroscopy (XPS), Fourier transformed infrared (FT-IR), powder X-ray diffraction (XRD), temperature programmed desorption of NH_3 (TPD of NH_3), temperature programmed desorption of CO_2 (TPD of CO_2), Raman spectroscopy, temperature programmed reduction (H_2-TPR), electron spin resonance (ESR), differential thermal and thermogravimetric analysis (DT/TGA), BET-surface area (BET-SA), CHNS and O_2 pulse chemisorption studies. The kinetic data obtained during the dehydrocyclization reaction includes, effect of calcination temperature of Zn–Cr–O, influence of glycerol concentration, in situ/ex situ treatments and poisoning of Zn–Cr–O catalyst with pyridine and 2,6-dimethylpyridine. The activity data was recorded after 6 h of continuous operation although the

* Corresponding author. Tel.: +91 40 27191720/+91-40-27193510; fax: +91 40 27160921.
E-mail address: akula@iict.res.in (A. Venugopal).

0926-860X/$ – see front matter © 2013 Elsevier B.V. All rights reserved.
http://dx.doi.org/10.1016/j.apcata.2013.10.023

steady-state activity was reached within 30 min. Nature and activity of Zn–Cr–O was described in concurrence with dehydrocyclization activities in relation with product distribution and their physicochemical characteristics particularly acid-base properties.

2. Experimental

2.1. Preparation of catalysts

The Zn–Cr–O catalyst employed in this investigation was prepared by a simple co-precipitation method using $Zn(NO_3)_2{\cdot}6H_2O$ and $Cr(NO_3)_3{\cdot}9H_2O$ (Sigma-Aldrich) with Zn:Cr = 2:1 (mole ratio), in order to produce a hydrotalcite structure [2]. The sample was prepared at a constant pH of 9 using a mixture of 2 M NaOH + 1 M Na_2CO_3 (base mixture) as precipitating agent. The gel was washed thoroughly, filtered and oven-dried for 12 h at 120 °C, and calcined in static air at 400, 450, 550, 650 and 750 °C for 5 h. The calcined Zn–Cr–O samples were denoted as ZC400, ZC450, ZC550, ZC650 and ZC750, respectively. The residual Na contents in the ZC400, ZC450, ZC550, ZC650 and ZC750 samples were analyzed by AAS and was found to be 0.33, 0.34, 0.30, 0.34 and 0.31 wt%, respectively. All of these samples were then evaluated for dehydrocyclization of EDA and aqueous glycerol and a selection of representative samples were characterized by adsorption and spectroscopic techniques.

2.2. Characterization of catalysts

Experimental conditions for the measurement of BET surface area, XRD, Raman, XPS, TPR, O_2 pulse chemisorption and TPD of NH_3 analyses were similar as reported earlier [4]. The basicity of catalysts was estimated by TPD of CO_2 using an Auto Chem 2910 (Micromeritics, USA). In a typical method about 0.1 g of calcined Zn–Cr–O sample was reduced at 400 °C for 5 h in 5%H_2/Ar (v/v) at a flow rate of 30 mL min^{-1}. After reductive pre-treatment the sample was saturated with 10.18% CO_2 (balance helium) at 60 °C, at a flow rate of 50 mL min^{-1} and subsequently flushed with helium gas at 60 °C for 1 h. The TPD CO_2 measurements were carried out from 60 to 600 °C at a ramping rate of 10 °C min^{-1}. The amount of desorbed CO_2 was calculated using GRAMS/32 software. The Fourier transformed infrared spectra were recorded in KBr pellets using a Thermo Nicolet Nexus 670 spectrometer in the region of 4000–400 cm^{-1}. FT-IR spectra of air calcined at 450 °C/5 h fresh; reduced (calcined in air at 450 °C/5 h followed by reductively pre-treated in 5%H_2/Ar at 400 °C/5 h), and the pyridine adsorbed (calcined in air at 450 °C/5 h followed by reduction in 5%H_2/Ar at 400 °C/5 h and subsequently a dose of approximately 500 μmol of pyridine injected in 10 successive pulses with each pulse of 40 μL in N_2 stream 30 mL min^{-1} on to catalyst at a temperature of 350 °C and flushed with N_2 at 350 °C/1 h) and 2,6-dimethylpyridine adsorbed (calcined in air at 450 °C/5 h followed by reduction in 5%H_2/Ar at 400 °C/5 h and subsequently a dose of ~580 μmol of 2,6-dimethylpyridine injected in 10 successive pulses with each pulse of ~60 μL in N_2 stream 30 mL min^{-1} on to catalyst at a temperature of 350 °C and flushed with N_2 at 350 °C/1 h) ZC450 sample. After the required pretreatment and subsequent adsorption of the probe molecule the samples were immediately transferred into desiccators and the wafers were subjected to FT-IR analysis. The carbon contents in used catalysts (recovered after 6 h of continuous operation) were measured using a VARIO EL, CHNS analyser. For brevity the TPR pattern, TPD of NH_3 curve, XPS and Raman spectra of ZC450 sample is not shown in this paper as we have reported it earlier [4].

2.3. Activity measurements

The dehydrocyclization activities on calcined and/or reduced Zn–Cr–O catalysts were performed in the temperature range of 300 to 400 °C and atmospheric pressure in a fixed-bed vertical quartz reactor (i.d = 8 mm, length = 450 mm) placed in a two zone furnace operated in a down flow mode. The first zone was preheating, which was maintained at 300 °C, and the second zone was the catalyst bed temperature, both monitored by a temperature controller-cum-programmer using a K-type thermocouple. Glycerol (Fluka) and EDA supplied by SDFCL, India were used. Nitrogen (IOLAR-I grade, BOC, India) was used as a carrier gas. The catalytic activities were carried out using −18/+23 sieved (BSS) catalyst particles. The carbon mass balance was done based on the inlet and outlet concentration of the organic moiety. Prior to the reaction, about 0.2 g of calcined catalyst (sieved particles −18/+25 BSS) was reduced in 5% H_2/Ar using 30 mL min^{-1} at 400 °C for 5 h. The catalytic activities were measured under strict kinetic control. An aqueous glycerol solution (20 wt% in H_2O) was used with a glycerol to EDA mole ratio of 1:1, at a flow rate of 5 mL h^{-1} (10 mmol glycerol + 10 mmol EDA + 200 mmol H_2O), along with N_2 as the carrier gas at a flow rate of 1800 mL h^{-1}. The reaction mixture contained a glycerol:EDA:H_2O:N_2 = 1:1:20:8 mole ratio. In some cases the flow rates were maintained at 8, 12 and 15 mL h^{-1}. In order to assess the nature of surface acid-base sites on dehydrocyclization activity of ZC450; pyridine (Bronsted and Lewis acid site blocker) and 2,6-dimethylpyridine (selective Bronsted acid site blocker) were used as probes. About 0.2 g of ZC450 sample was reduced in 5%H_2/Ar at 400 °C/5 h followed by a dose of 500 μmol of pyridine in 10 successive pulses in a time interval of 10 min injected into the stream using 30 mL min^{-1} of N_2 as carrier gas at a temperature of 350 °C. After the pyridine adsorption the sample was flushed with N_2 at 350 °C for 1 h subsequently the reaction was carried out using a reaction mixture that contained glycerol:EDA:H_2O:N_2 = 1:1:20:8 mole ratio and the liquid mixture (glycerol + EDA + H_2O) flow rate of 5 mL h^{-1}. Similar protocol was maintained while using about 580 μmol of 2,6-dimethylpyridine as another probe in 10 successive pulses in a time interval of 10 min injected into the stream. The product mixture was analyzed by gas chromatograph (Shimadzu, GC-17A) via a flame ionization detector (FID) using a ZB-5 capillary column at a ramping rate of 10 °C min^{-1} from 60 to 280 °C. The mass balance for all the measurements was >95%. The samples were analyzed by GC–MS (QP5050A Shimadzu) using a ZB-5 capillary column with EI mode (SI).

3. Results

3.1. BET-surface area and XRD analysis

The BET-surface areas of Zn–Cr–O samples are reported in Table 1. Surface area of the Zn–Cr–O sample drastically decreased from 76.5 to 21.6 m^2 g^{-1} with the increase in calcination temperature from 400 to 750 °C. XRD patterns of the Zn–Cr–O oven dried sample (SI) exhibited diffraction data characteristic of the hydrotalcite structure and upon calcination in static air at various temperatures ranged between 400 and 750 °C (Fig. 1) showed reflections attributed to ZnO [ICDD no. 89-0510] and $ZnCr_2O_4$ [ICDD no. 22-1107] phases [4–6]. Peaks due to neither ZnO nor $ZnCr_2O_4$ phases were identified with ZC400, probably due to amorphous nature or the crystallite size below the X-ray detection limit. Generation of very fine $ZnCr_2O_4$ spinel increases the surface area by suppressing the crystal growth of ZnO, but formation of large sized $ZnCr_2O_4$ spinels leads to lowering of the surface area due to unsuppressed ZnO crystal growth [7]. The average crystallite size of ZnO and $ZnCr_2O_4$ were measured using Scherrer formula and the data is reported in Table 1. Fig. 1 shows an increase in resolution of ZnO and $ZnCr_2O_4$ peaks and the crystallite size of ZnO and $ZnCr_2O_4$ phases at high calcination temperature. At low calcination temperatures ~400 °C, formation of neither zinc chromite nor ZnO phases

Table 1
Physicochemical properties of Zn–Cr–O samples calcined from 400 to 750 °C in static air.

Sample	S_{BET} ($m^2\ g^{-1}$)	Uptake ($\mu mol\ m^{-2}$)				[e]Crystallite size (nm)	
		[a]H_2	[b]O_2	[c]NH_3	[d]CO_2	ZnO (1 0 0)	$ZnCr_2O_4$ (3 1 1)
ZC400	76.5	3.75	1.82	5.7	18.6	nd	nd
ZC450	38.9	2.68	1.77	2.6	25.2	19.8	14.5
ZC550	36.6	2.55	1.37	2.4	19.7	33.1	16.5
ZC650	26.2	2.37	1.27	2.4	4.3	37.8	21.9
ZC750	21.6	2.51	1.42	1.8	5.0	42.9	32.9

[a] H_2 uptake measured by TPR analysis calibrated with TPR of Ag_2O.
[b] O_2 uptake measured by pulse chemisorption at 335 °C.
[c] NH_3 uptake measured by TPD of NH_3.
[d] CO_2 uptake measured by TPD of CO_2.
[e] Crystallite size of ZnO and $ZnCr_2O_4$ measured using Scherrer formula.

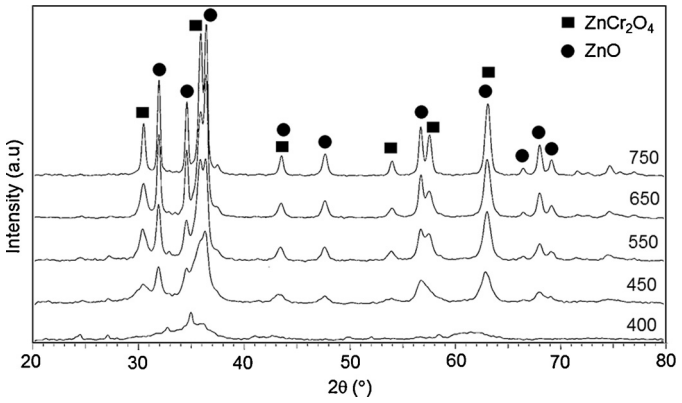

Fig. 1. XRD patterns of the Zn–Cr–O sample calcined in air at various temperatures.

are observed. Pre-existence of amorphous hydroxy zinc chromate phase may be possible over Zn–Cr–O when the sample is calcined ≤400 °C [8]. The DT/TGA analysis of the oven dried Zn–Cr (HT) sample revealed no weight loss above 400 °C (SI).

3.2. TPR analysis

TPR patterns of Zn–Cr–O sample calcined in air from 400 to 750 °C are presented in Fig. 2 and the H_2 uptakes are reported in Table 1. Two observations were clear from the patterns, firstly the T_{max} is shifted towards high temperatures and secondly H_2 uptakes were decreased with increase in calcination temperature of Zn–Cr–O catalyst. The shift in T_{max} towards high temperatures suggests that the oxygen is more strongly bound as chromate species in the high temperature calcined samples [9]. The decrease in H_2 uptake with increase in calcination temperature may be explained based on two possibilities; (i) due to the increased crystallite size of ZnO and $ZnCr_2O_4$ species as observed from XRD analysis. (ii) May be due to eventual conversion of Cr^{6+} to Cr^{3+} species to certain extent

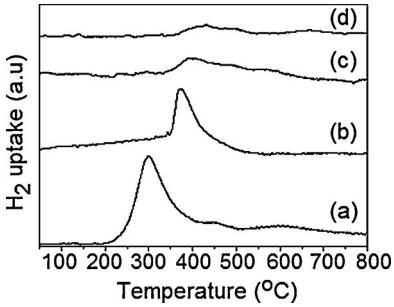

Fig. 2. H_2-TPR patterns of Zn–Cr–O sample calcined in air at a temperature of (a) 400 (b) 550 (c) 650 (d) 750 °C samples.

during the decomposition of surface chromate ($ZnCrO_4$) species with rise in calcination temperature [8,10]. A small tail extending peak appeared above 450 °C is probably due to strongly interacted ZnO and Cr–O species in the catalyst. Higher H_2 uptake over ZC400 than the others is either probably because of relatively high concentration of surface chromate species or existence of amorphous Cr–O oxide species.

3.3. FT-IR analysis

IR spectra of spinels are characterized by four bands which originate due to F_{1u} symmetry. The band recorded around 627 cm^{-1} in all the fresh and reduced samples is due to ν_1 mode and a broad band at 504 cm^{-1} is due to mode ν_2. These bands at 504 and 627 cm^{-1} correspond to the vibrations of ZnO_4 tetrahedra and octahedra of complexes of tri-valent chromium atom with oxygen (Fig. 3a). The occurrence of these bands indicates the spinel structure of $ZnCr_2O_4$ [11]. Upon increasing the calcination temperature of Zn–Cr–O sample; the band intensities at 504 and 627 cm^{-1} have increased. The broadness of 504 cm^{-1} band with shoulder band centred at 530 cm^{-1} (Fig. 3a) may probably due to weakening of the M–O bond. The intensity of shoulder peak at 530 cm^{-1} increased with increase in calcination temperature in the spinel structure which is more pronounced at high temperature calcined samples. The bands at 933–928 and 952 cm^{-1} are characteristic of the vibrations of CrO_4 tetrahedra due to Cr^{6+} ions [11]. Fig. 3b shows the presence of Cr^{6+} species in fresh Zn–Cr–O samples in the band region 933–928 and 952 cm^{-1} and their intensities decreased with increase in calcination temperature of Zn–Cr–O. Decrease in peak intensities of Cr^{6+} is probably due to partial reduction of Cr^{6+} to Cr^{3+} at elevated temperatures. Similar results were reported by Fahim et al. when ZnO–$ZnCr_2O_4$ sample was subjected to high temperature treatment and it was further confirmed from the surface chromate estimations of Zn–Cr mixed oxides by Pirogova et al. [8,10]. Formation of the intermediate hydroxy zinc chromate seems to occur with Zn–Cr–O sample calcined at relatively low temperatures i.e. ≤400 °C. These chromate species are easily reducible in H_2 stream at 400 °C as can be seen from the disappearance of the bands typical (Fig. 3b) for the vibrations of CrO_4 tetrahedra at 933–928 and 952 cm^{-1} due to reduction of $Cr^{6+} \rightarrow Cr^{3+}$. TPR analysis revealed the lower H_2 uptakes on high temperature calcined samples which corroborate this observation.

3.4. XPS analysis

The X-ray photoelectron spectra of Zn–Cr–O fresh samples exhibited (Fig. 4a) O1s lines in the region 529.9 to 532.7 eV that are attributed to signal contributions from two types of oxygen containing species in the near surface region. All the samples showed a second peak in the region 532.1 to 532.7 eV which demonstrates the presence of oxygen with two contributions. The Zn2p BE

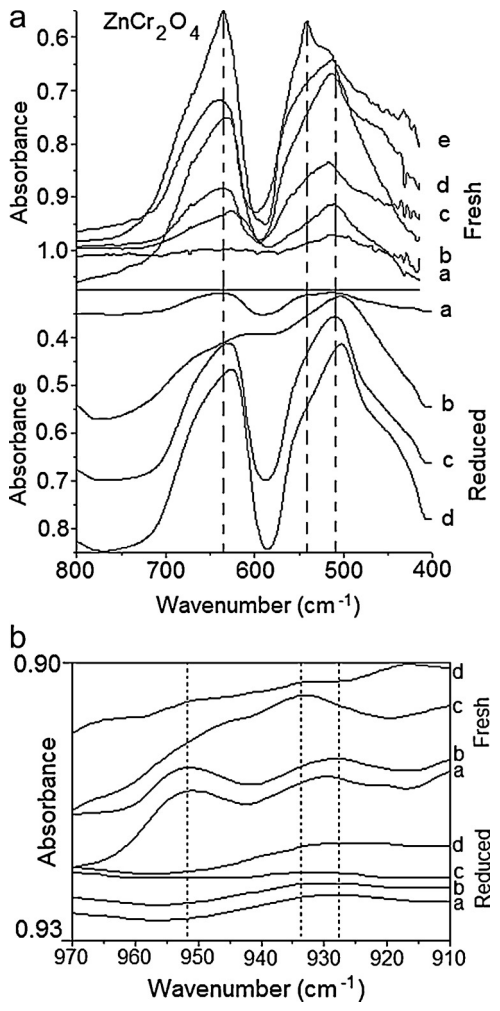

Fig. 3. (a) FT-IR spectra of fresh Zn–Cr–O calcined in air at a temperature of (a) 400 (b) 450 (c) 550 (d) 650 (e) 750 °C and reduced in 5%H_2/Ar at 400 °C/5 h. (b) FT-IR spectra of fresh Zn–Cr–O calcined in air at a temperature of (a) 400 (b) 450 (c) 550 (d) 650 °C and reduced in 5%H_2/Ar at 400 °C/5 h.

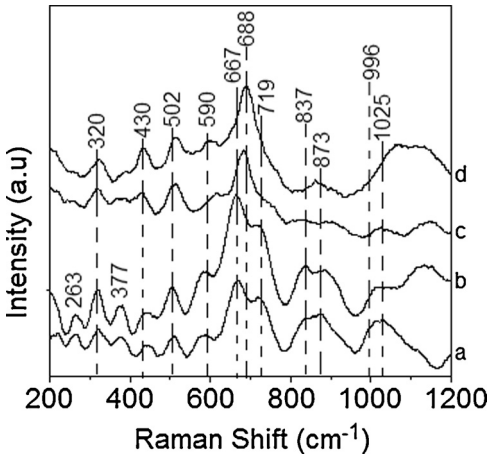

Fig. 5. Raman spectra of fresh Zn–Cr–O sample calcined in air at a temperature of (a) 400 (b) 550 (c) 650 and (d) 750 °C sample.

values of 1021.5 to 1022.2 eV are characteristic of ZnO and $ZnCr_2O_4$, respectively (Fig. 4b). The primary state of Zn in the near surface region of these catalysts is ZnO and $ZnCr_2O_4$. The spectra shows Cr 2p peaks centred at 576.3 to 576.7 eV, attributed to Cr^{3+} species for ZC400, ZC550, ZC650 and ZC750 catalysts, respectively [5,12,13]. The peak at 578.1 eV ascribed to Cr^{6+} species shifted to 576.3 eV in ZC400 to ZC750 samples (Fig. 4c) denoting the transition of Cr^{6+} to Cr^{3+}. These observations are in good agreement with earlier reports of XPS analysis of ZnO–$ZnCr_2O_4$ mixed oxide catalysts [14,15]. Shift in Cr 2p peak towards low BE was clearly seen on high temperature treated samples ZC600 and ZC700, which could be due to auto reduction of Cr^{6+} to Cr^{3+} species in air calcination at high temperatures. It was further evident from FT-IR spectra of high temperature calcined samples (Fig. 3b) which indicated the diminished band intensities at 952 and 932–938 cm^{-1} attributed to partial reduction of Cr^{6+} to Cr^{3+}.

3.5. Raman spectra of Zn–Cr–O

Raman spectra of Zn–Cr–O calcined in the temperature range 400 to 750 °C are collected at room temperature and reported in Fig. 5. Spectra show two prominent bands at 260, 370 cm^{-1} that appeared in ZC400 and ZC550 and not seen in ZC650 and ZC750 samples. The peak at 320 cm^{-1} (Fig. 5) is the vibration mode

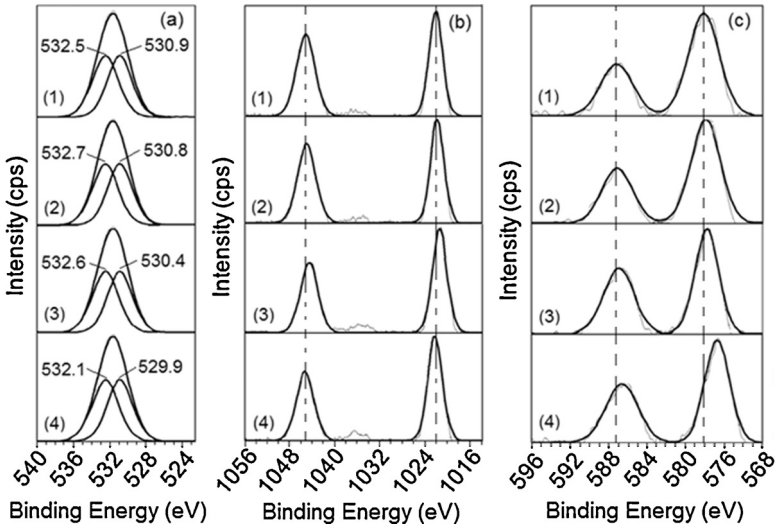

Fig. 4. XPS analysis (a) O1s (b) Zn2p (c) Cr2p spectra of Zn–Cr–O calcined in air at various temperatures (1) 400 (2) 550 (3) 650 and (4) 750 °C samples.

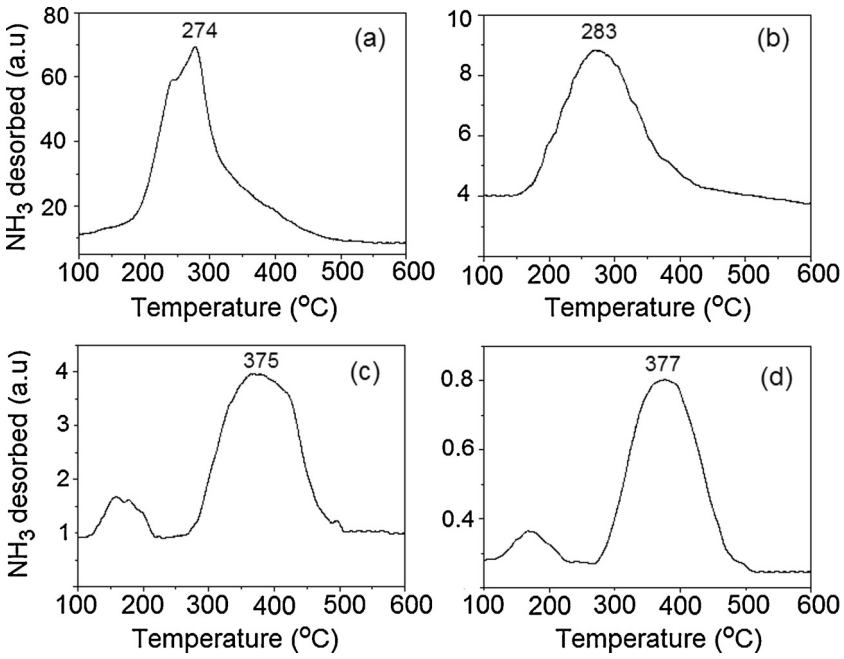

Fig. 6. TPD of NH_3 patterns of Zn–Cr–O calcined in air at a temperature of (a) 400 (b) 550 (c) 650 and (d) 750 °C sample.

associated with the multiple-phonon scattering processes of ZnO. Broad peak at 430 cm^{-1} may be due to E_2 phonon frequency of ZnO as expected from Raman selection rules in semiconductors with wurtzite crystal structure [4] or it may be due to phonon band originated because of E_g symmetry of spinel. Fig. 5 also shows strong bands between 500 and 800 cm^{-1}. Peak with medium intensity located at 502 cm^{-1} has the F_{2g} symmetry. The band at 590 cm^{-1} of the F_{2g} mode in this region is not well separated because of its lower intensity. The intense Raman band at 667–688 cm^{-1} is the symmetric Cr–O stretching vibration of CrO_6 groups of spinel originated due to A_{1g} symmetry. Its broadness is related to cation-anion bond lengths and polyhedral distortion in $ZnCr_2O_4$ [16]. Such distortion is more prominent in ZC400 and ZC550 compared to ZC650 and ZC750 samples. In a spinel structure CrO_6 is regular only for ideal geometry and distortion is present in CrO_6 group, consequently symmetry is lowered as result additional Raman bands appeared in the case of ZC400 and ZC550 in contrast to ZC650 and ZC750 samples. Bands observed in the region 1000–800 cm^{-1} are ascribed to Cr^{6+} species in the form of chromates. The bands that appeared at 837 cm^{-1} are low in intensities with high temperature calcined samples [17]. The intensity of characteristic Cr=O (Cr^{6+}) stretching vibration of Raman band at around 996 cm^{-1} decreased with increase in calcination temperature further indicating the reduction of Cr^{6+} species of Zn–Cr–O samples. These findings are in good agreement with earlier reports [18]. These results demonstrated that the ZnO is found to be in wurtzite crystal lattice whereas $ZnCr_2O_4$ is in a spinel form contained with deformation modes that conceived several Raman bands. Upon high temperature treatment the Cr^{6+} species in Zn–Cr–O sample is reduced to some magnitude as was clearly evidenced from TPR, FT-IR, XPS and Raman analyses.

3.6. O_2 pulse chemisorption studies

The O_2 uptakes of Zn–Cr–O sample calcined in the temperature range 400 to 750 °C are reported in Table 1. O_2 uptake is the measure of extent of surface re-oxidation of the reducible or partially reducible mixed metal oxide catalysts. The O_2 uptakes were gradually decreased with increase in calcination temperature of the Zn–Cr–O catalyst. Presence of higher number of surface chromate species in ZC400 may be a reason for higher O_2 uptake than the other samples [8].

3.7. TPD of NH_3 and CO_2 studies

The acid-base strengths of the Zn–Cr–O samples are estimated by TPD of NH_3 and TPD of CO_2 analyses and the results are reported in Table 1. When the specific uptakes are compared it is evident (Table 1) that both NH_3 and CO_2 uptakes are decreased with increase in calcination temperatures. Fig. 6 represents the NH_3 desorption curves of Zn–Cr–O samples which displayed the shift in T_{max} (~100 °C) towards high temperatures upon calcination at high temperatures. Contrary to this TPD of CO_2 curves (Fig. 7) indicated that the T_{max} was slightly shifted to low temperatures. TPD studies demonstrate that total number of acid sites decreased although small amount of strong acid sites were generated at high calcination temperatures. In analogy total basicity of the Zn–Cr–O catalysts decreased but reverse trend is noticed by the formation of moderate to strong basic sites as the T_{max} was shifted to slightly low temperatures. Decrease in acid-base strength at high temperature treated catalysts may be explained due to increased crystallite size

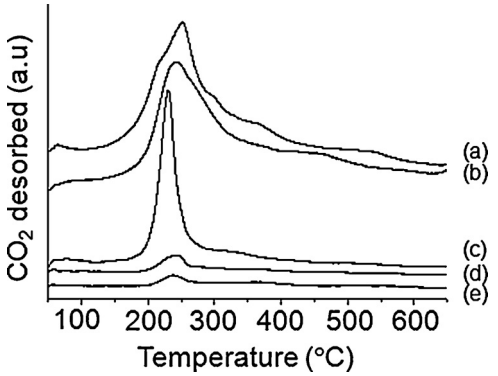

Fig. 7. TPD of CO_2 patterns of Zn–Cr–O calcined in air at a temperature of (a) 400 (b) 450 (c) 550 (d) 650 and (e) 750 °C sample.

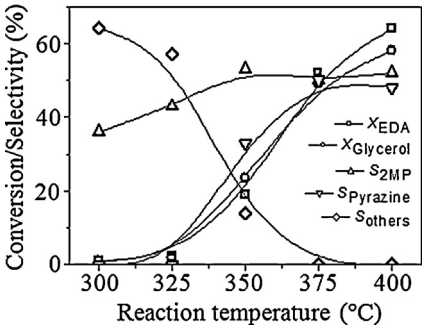

Fig. 8. Dehydrocyclization of glycerol and EDA over fresh Zn–Cr–O calcined in air at 400 °C/5 h using a reaction mixture flow rate of 5 mL h^{-1}, GHSV = 9.37 mL g_{cat}^{-1} s^{-1}, glycerol:EDA:H_2O:N_2 = 1:1:20:8 (mole ratio).

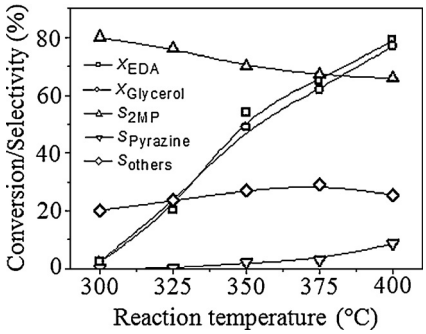

Fig. 9. Dehydrocyclization of glycerol and EDA over Zn–Cr–O calcined in air at 400 °C/5 h and reduced in 5%H_2/Ar flow rate of 30 mL min^{-1} at 400 °C/5 h using a reaction mixture flow rate of 5 mL h^{-1}, GHSV = 9.37 mL g_{cat}^{-1} s^{-1}, glycerol:EDA:H_2O:N_2 = 1:1:20:8 (mole ratio).

(Table 1) of both ZnO and $ZnCr_2O_4$ species that was further evident from the lower O_2 uptakes on ZC650 and ZC750 samples.

3.8. Activity measurements

3.8.1. Dehydrocyclization of EDA and aqueous glycerol over fresh calcined ZC400

Conventionally 2-methylpyrazine is synthesized by dehydrocyclization of EDA and 1,2-propyleneglycol over Pd-ZnO–$ZnCr_2O_4$ catalysts [19]. First time we have reported the synthesis of 2MP using EDA and glycerol and a reaction mechanism was proposed via dehydrocyclization through a cyclic transition state due to homocoupling of 2-pyrazinylmethanol [2]. The dehydrocyclization is carried out in the temperature range of 300 to 400 °C over air calcined Zn–Cr–O (ZC400) sample and the data is reported in Fig. 8. The conversion of glycerol and EDA are low (<5%) upto a reaction temperature of 325 °C; from there onwards it is quite detrimental and the curve is light off nature. At low reaction temperatures 2MP was low and selectivity towards other by-products includes acetone, dihydroxyacetone that were too high. This indicates that the reaction does seem to precede by dehydration of glycerol rather than dehydrocyclization with EDA at low reaction temperatures. Maximum selectivity towards 2MP was 53% at 350 °C. At a reaction temperature of 400 °C; selectivity towards pyrazine is almost 40% with 7% of by-products includes 2-pyrazinealdehyde, 2-pyrazinylmethanol, 2,3- and 2,5-dimethylpyrazines. High ratio of pyrazine may be because of three possible reasons, firstly by disproportionation of 2MP, secondly by intermolecular cyclization of EDA [20] and finally by hydrogenolysis of C–C in 2MP (schemes see SI).

High selectivity of pyrazine is rationalized based on the fact that if one would assume that the reaction proceeds via 2MP disproportionation mechanism; equal molar proportions of pyrazine and dimethylpyrazines are expected. On the contrary almost constant selectivity of 2MP (Fig. 8) in the temperature range from 350 to 400 °C elucidate that disproportionation mechanism can be ruled out because of very low amounts of dimethylpyrazines were obtained. Another possibility by intermolecular cyclization of EDA cannot be considered for the reason that conversion of EDA and glycerol are in equal proportions and no other by-products that could be expected from glycerol alone was observed in the product mixture in the reaction temperature from 350 to 400 °C. Therefore, the high ratio of pyrazine may possibly due to hydrogenolysis reaction on the unreduced Zn–Cr–O surface. Thus it can be concluded that at reaction temperature above 325 °C; both conversion of EDA and glycerol and selectivity of 2MP are reasonably good but the enhanced selectivity of pyrazine at high reaction temperatures is due to hydrogenolysis reaction on the unreduced Zn–Cr–O sample (ZC400).

3.8.2. Dehydrocyclization of EDA and aqueous glycerol over reduced ZC400

The dehydrocyclization is performed over ZC400 sample after a reductive pretreatment in H_2/Ar at 400 °C/5 h prior to the reaction and the results are reported in Fig. 9. The reduced Zn–Cr–O (ZC400) catalyst showed about 75% of EDA and glycerol conversions with 67% selectivity towards 2MP along with 10% pyrazine. At a reaction temperature of 400 °C; 2MP rate is 39.4 and 23.4 μmol s^{-1} m^{-2} on reduced and unreduced ZC400 catalyst, respectively. Thus suggesting the dehydrocyclization of EDA and glycerol requires a reductive pretreatment of Zn–Cr–O catalyst for better 2MP yields. The Zn–Cr–O reduced in H_2 seems to create additional surface energetic domains active for dehydrocyclization reaction.

The $T_{1/2}$ (temperature at which 50% of glycerol was converted) is found to be 354 °C on reduced ZC400 with a 2MP selectivity ~70%; whereas ZC400 showed 50% 2MP selectivity at $T_{1/2}$ = 381 °C without reductive pretreatment (SI). The 2MP rates were compared under reduced and unreduced conditions on ZC400 sample and the data is reported in Fig. 10. In the temperature range 325 to 400 °C rate of 2MP is 2 times higher on reduced than on unreduced Zn–Cr–O sample. The unreduced surface of Zn–Cr–O usually possess high amount of labile/surface oxygen than on the reduced surface. Lower 2MP yields on unreduced Zn–Cr–O may be due to the presence of electronically coupled Cr(III)–Cr(VI)–O species in close proximity to $ZnCr_2O_4$ species [4]. Surface oxygen seems to play some role on the dehydrocyclization activity of reduced and unreduced Zn–Cr–O surface. The nature and strength of surface oxygen is explained by O_2 pulse chemisorption studies on bulk ZnO, Cr_2O_3 and $ZnCr_2O_4$ oxides in conjunction with characteristics of Zn–Cr–O in order to establish the differences in dehydrocyclization activities.

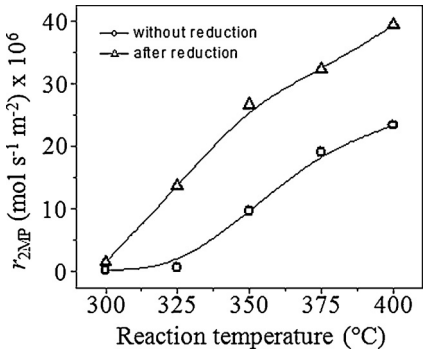

Fig. 10. Comparison of 2MP rates over fresh and reduced Zn–Cr–O (ZC400) catalyst in the dehydrocyclization of glycerol and EDA at a flow rate of 5 mL h^{-1}, GHSV = 9.37 mL g_{cat}^{-1} s^{-1}, glycerol:EDA:H_2O:N_2 = 1:1:20:8 (mole ratio).

Table 2
Dehydrocyclization of glycerol and EDA over bulk ZnO, Cr_2O_3 and $ZnCr_2O_4$ catalysts.

Sample	[a]O_2 uptake (μmol m^{-2})	O atom (nm^{-2})	[b]X_{EDA}	[b]$X_{glycerol}$	[b]r_{2MP} (μmol s^{-1} m^{-2})	[b]$r_{2\text{-pyrazinylmethanol}}$ (μmol s^{-1} m^{-2})
ZnO	0.045	0.054	58.9	62.1	29.2	9.8
Cr_2O_3	0.825	0.994	36.5	10.5	0.3	0.006
$ZnCr_2O_4$	0.916	1.103	32.1	31.6	41.3	4.8

[a] Ref. [4].
[b] This work.

3.8.3. Comparative studies over bulk ZnO, Cr_2O_3 and $ZnCr_2O_4$ catalysts in dehydrocyclization of EDA and aqueous glycerol

The dehydrocyclization activity on bulk ZnO, Cr_2O_3 and $ZnCr_2O_4$ samples was carried out under standard conditions and the data is reported in Table 2. Due to synergetic interaction between two different metal oxides; the mixed oxides frequently show better catalytic performance than their individual components. Inspection of the Table 2 revealed that bulk ZnO showed better 2MP rate than on bulk Cr_2O_3. The bulk Cr_2O_3 promoted intermolecular cyclization of EDA to produce pyrazine [20]. Although the EDA and glycerol conversions were moderate; 2MP rate was 2 orders of magnitude higher over ZnO than on Cr_2O_3. The bulk $ZnCr_2O_4$ showed better 2MP yields than the ZnO. Therefore it is inferred that presence of chromium in ZnO matrix in the form of spinel structure seems to promote the dehydrocyclization reaction as bulk Cr_2O_3 catalyst displayed the intermolecular cyclization of EDA to produce pyrazine [4].

The reduced surface of Zn–Cr–O mixed metal oxides prevails in coordinative unsaturated cations (Lewis acid) and Lewis basic sites (oxide anion). Subsequent exposure of these reduced surfaces to H_2O (as the reaction mixture contained large amounts of H_2O along with glycerol and EDA) at moderate temperatures ($300 < t < 400\,^{\circ}C$) convert the surface Lewis acid sites into Bronsted acid sites to certain magnitude nevertheless it depends on the surface local environment [21]. It should be mentioned here that O_2 uptake on bulk ZnO is (0.045 μmol m^{-2}) which is 2.4% of the O_2 uptake on ZC400 (1.82 μmol m^{-2}) sample. Hence the charge balance by surface oxygen on Zn–Cr–O surface mostly contributed from Cr_xO_y species rather than ZnO. The O_2 uptake measured by pulse chemisorption is considered as a measurement of surface redox species in contrast to H_2 uptakes attributed to Cr_xO_y species estimated by TPR method which is a bulk analysis. The O_2 uptakes on bulk and mixed oxides revealed (Table 2); a 20 times higher O_2 uptake on $ZnCr_2O_4$ than on ZnO suggests that chromium species demarcate the limit of O_2 adsorption on ZnO–$ZnCr_2O_4$ mixed oxide (Table 1) as approximately 40 times higher O_2 uptake was observed on ZC400 sample.

3.8.4. Influence of calcination temperature of Zn–Cr–O in the dehydrocyclization of EDA and aqueous glycerol

The activity data obtained on reduced surface (usually possess higher number of coordinatively unsaturated sites) showed better 2MP yields, whereas the unreduced Zn–Cr–O surface (Cr^{6+} rich: abound by lower number of coordinatively unsaturated sites) exhibited lower 2MP yields. The ESR spectra of both fresh and reduced Zn–Cr–O sample [see SI] did not show signals attributed to Cr^{5+} except the other paramagnetic Cr^{3+} species. Hence the Zn–Cr–O sample was calcined in air at various temperatures from 400 to 750 °C (denoted as ZC400, ZC450, ZC550, ZC650, ZC750) and subjected to reductive pretreatment (in 5%H_2/Ar at 400 °C/5 h) prior to reaction and the data is reported in Fig. 11. Based on the product distribution and conclusions drawn from the above results a plausible surface reaction mechanism has been proposed and reported in Scheme 1.

Both glycerol and EDA conversions were decreased upon increasing calcination temperature of Zn–Cr–O (Fig. 11). Product

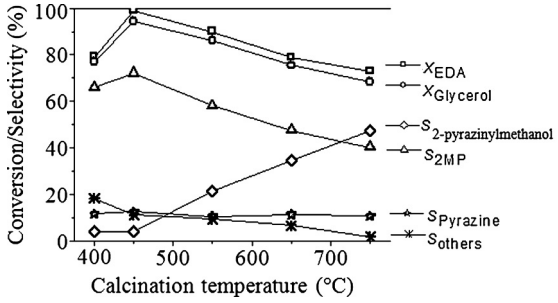

Fig. 11. Influence of calcination temperature on Zn–Cr–O samples (reduced in 5%H_2/Ar at 400 °C/5 h) in the dehydrocyclization of glycerol and EDA using a reaction mixture flow rate of 5 mL h^{-1}, GHSV = 9.37 mL g_{cat}^{-1} s^{-1}, glycerol:EDA:H_2O:N_2 = 1:1:20:8 (mole ratio).

distribution revealed that 2MP was major (40% to 72%) with ~12% pyrazine and 4% to 47% of 2-pyrazinylmethanol along with 2% to 18% of dimethylpyrazines and 2-pyrazinaldehyde were observed. The ZC400 showed lowest 2MP rate *ca.* 20 μmol s^{-1} m^{-2}. The 2MP rate was considerably decreased with increase in calcination temperature from ca. 52.8 to 32.7 μmol s^{-1} m^{-2} conversely rate of 2-pyrazinylmethanol was significantly increased (Table 3). The enhanced rate of 2-pyrazinylmethanol on high temperature calcined samples could be possibly due to reduction in the rate of homo-coupling of 2-pyrazinylmethanol (Scheme 1) to form a cyclic transition state through which the 2MP and the pyrazinaldehyde are being formed. In contrast the dimethylpyrazines (2,3- 2,5- 2,6-) were slightly decreased with increase in calcination temperature from 400 to 750 °C (Fig. 11). Pyrazine is almost constant irrespective of calcination temperature. As reported earlier that pyrazine is expected via intermolecular cyclization of EDA over bulk Cr_2O_3 due to strong acid sites [4]. Liu et al. have observed high selectivity of 2-pyrazinylmethanol than the 2MP in the cyclocondensation of glycerol and EDA over Fe, Zn- modified SiO_2–Al_2O_3 catalysts [22].

Formation of 2MP and pyrazinaldehyde can also be expected by simultaneous hydrogen and dehydrogenation of 2-pyrazinylmethanol. Dehydrocyclization has been performed in the presence of H_2 over ZC650 sample so as to validate the simultaneous hydrogenation and dehydrogenation of 2-pyrazinylmethanol. Product distribution revealed that a slight increase in 2MP and decrease in 2-pyrazinaldehyde selectivity and 2-pyrazinylmethanol is unchanged. The enhanced 2MP selectivity is found to be at the cost of 2-pyrazinaldehyde. If the simultaneous hydrogenation and dehydrogenation reactions are anticipated then an equal proportion of 2MP and 2-pyrazinaldehyde is expected.

Table 3
Comparison of 2MP and 2-pyrazinylmethanol rates over Zn–Cr–O samples calcined at various temperatures.

Sample	r_{2MP} (μmol s^{-1} m^{-2})	$r_{2\text{-pyrazinylmethanol}}$ (μmol s^{-1} m^{-2})	Carbon (wt%)
ZC400	20.0	1.2	4.06
ZC450	52.8	3.1	1.95
ZC550	42.0	15.1	1.56
ZC650	35.8	25.9	1.54
ZC750	32.7	38.4	0.82

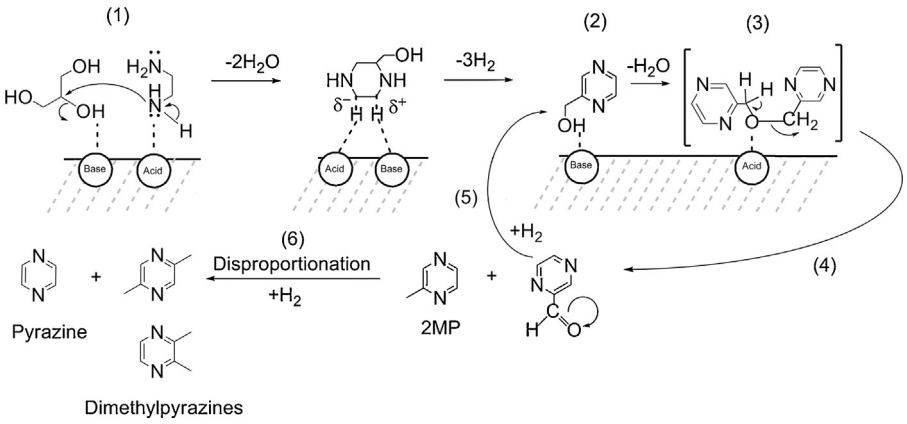

Scheme 1. Proposed surface reaction mechanism in the dehydrocyclization of glycerol and EDA.

Moreover selectivity of 2-pyrazinynaldehyde is less than 5% over all the catalysts tested at various reaction conditions. These results is an indication of the homo coupling of 2-pyrazinylmethanol to form a transition state through which 2MP and 2-pyrazinaldehyde are being formed [23–25].

The catalysts recovered after 6 h of use showed that decrease in carbon depositions (Table 3) with increase in calcination temperature of Zn–Cr–O. Thus suggests the carbon deposition is occurring mostly after the homo-coupling of 2-pyrazinylmethanol. Higher 2MP rates on ZC450 sample rendered us to extend some kinetic studies to further evaluate the nature of ZC450 sample. The time on stream analysis on ZC450 sample (SI) showed steady activity upto 48 h continuous operation with sustained 2MP rate.

3.8.5. Dehydrocyclization activity at various GHSV over reduced ZC450

The dehydrocyclization studies on ZC450 sample has been carried out at various GHSV and the results are reported in Fig. 12. Upon increasing the space velocity; conversion of both EDA and glycerol were decreased; as a result 2MP yield was decreased. It is probably due to decrease in contact time. It is interesting to note that selectivities towards 2-pyrazinylmethanol was slightly increased at higher space velocities. These results denote that the rate of 2MP is dependent on the conversion of 2-pyrazinylmethanol to transform (Scheme 1) into 2MP and 2-pyrazinaldehyde. From this it can be concluded that the rate of 2MP is dependent on homo-coupling of 2-pyrazinylmethanol.

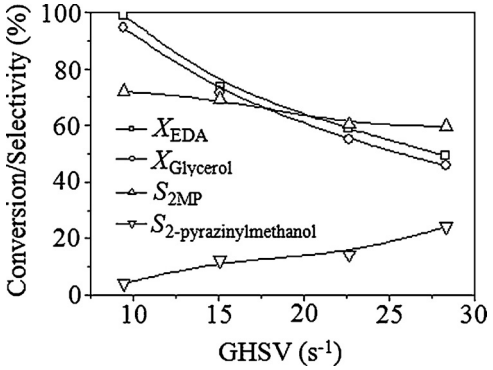

Fig. 12. Comparison of 2MP and 2-pyrazinylmethanol formation at higher flow rates in the dehydrocyclization of glycerol and EDA over reduced (5%H_2/Ar flow rate = 30 mL min^{-1} at 400 °C/5 h) ZC450 catalyst. Flow rate of reaction mixture = 5, 8, 12, 15 mL h^{-1}, GHSV = 9.37 to 28.1 mL g_{cat}^{-1} s^{-1}, with a mole ratio of glycerol:EDA:H_2O:N_2 = 1:1:20:8.

3.8.6. Activity measurements using pure EDA and pure glycerol over reduced ZC450

In order to substantiate these issues the ZC450 sample has been evaluated using various compositions of reaction mixtures and the data is presented in Table 4. The activity data shows that using aqueous glycerol; dehydration products such as 3-hydroxypropionaldehyde ~60% with 2-oxopropanal (30%) and hydroxyacetone (10%) were observed. Such products are usual intermediate by-products observed in the hydrogenolysis of aqueous glycerol over $CuCr_2O_4$ catalysts in H_2 at very high pressures [26]. This product distribution indicates that two types of active sites (i) dehydration and (ii) dehydrogenation are present on the catalyst surface [SI]. In presence of aqueous EDA the ZC450 showed intermolecular cyclization activity to produce only pyrazine. In order to verify the disproportionation of 2MP, the ZC450 has been examined at very high reaction temperature of 450 °C using 20 wt% of 2MP in H_2O and found that minute 2MP conversion (~0.5%) was observed with 99.9% selectivity of pyrazine indicates the reaction followed by hydrogenolysis of 2MP (Table 4). The dehydrocyclization is also examined using pure EDA and pure glycerol mixture (1:1 mole ratio) at 400 °C and identified about 38.5% of 2-pyrazinylmethanol with 45% 2MP selectivity. A high ratio of 2-pyrazinylmethanol in the absence of H_2O using pure EDA and glycerol suggests that dehydrocyclization requires certain amount of H_2O; which seems to generate surface hydroxy groups at ≥300 °C on the catalyst surface. The drastic reduction in 2MP selectivity upon using pure substrates prompted us to investigate the dehydrocyclization activity on ZC450 using various loadings of glycerol in the range 5 to 30 mmol in H_2O.

3.8.7. Effect of glycerol loading in dehydrocyclization of EDA and aqueous glycerol over reduced ZC450

Effect of glycerol loading was carried out using 1:1 mole ratio of glycerol to EDA at a reaction temperature of 400 °C (GHSV ~ 9.37 mL g_{cat}^{-1} s^{-1}) and the data is reported in Fig. 13. It shows that the conversion of EDA and glycerol were slowly dropped upto a glycerol loading of 18 mmol and from there onwards it is quite low. On the other hand pure EDA and pure glycerol showed very poor conversions (Table 4). These results pointed out that certain amount of H_2O is required for dehydrocyclization of glycerol and EDA. It appears that under the reaction conditions (≥300 °C) surface regenerates hydroxy groups after reductive pretreatment. These hydroxy groups are either acid or base (Bronsted and/or Lewis) in nature. The nature of surface hydroxy groups is established by adsorption of two different Lewis bases prior to dehydrocyclization of glycerol and EDA.

Table 4
Activity measurements using various feed compositions over reduced ZC450 sample at a reaction temperature of 400 °C; flow rate = 5 mL h^{-1}.

[a]Feed composition	X_{EDA}	$X_{gly.}$	S_{2MP}	$S_{pyrazine}$	$S_{2\text{-pyrazinylmethanol}}$	S_{others}
(1) 20 wt% aq. glycerol	–	3.7	0.0	0.0	0.0	(i) Hydroxypropionaldehyde = 60% (ii) 2-oxopropanal = 30% (iii) Hydroxyacetone = 10%
(2) 20 wt% aq. EDA	5.2	–	0.0	100	0.0	0.0
(3) 20 wt% aq. 2MP %Conv. = 0.5	–	–	–	99.9[b]	0.0	0.0
(4) Pure EDA + pure glycerol (1:1 mole ratio)	4.6	3.8	45.0	10.6	38.5	(i) Dimethylpyrazines = 3.8 (ii) Pyrazinaldehyde = 2.1

[a] Reaction temperature = 400 °C.
[b] Reaction temperature = 450 °C.

3.8.8. Dehydrocyclization of EDA and aqueous glycerol under poisoning conditions

The 2,6-dimethylpyridine will be selectively adsorbed on Bronsted acid site due to steric hindrance posed by methyl groups in 2nd and 6th position and pyridine can be adsorbed on both Bronsted and Lewis sites. Influence of surface acid-base sites on the dehydrocyclization activities is examined by poisoning the catalysts with pyridine and 2,6-dimethylpyridine as a probes [27]. Prior to reaction the ZC450 sample was reduced in 5%H_2/Ar at 400 °C/5 h and the sample was flushed with N_2 (at a flow rate of 30 mL min^{-1} for 3 h at 400 °C) subsequently pyridine of about 500 μmol (in 10 successive pulses in a time interval of 10 min) adsorbed in N_2 stream at 350 °C followed by flushing of the sample again in N_2 flow at 350 °C/1 h. After the consecutive treatments and pyridine adsorption the catalyst was subjected for activity measurements at a flow rate of 5 mL h^{-1} and reaction temperature of 350 °C. Similar protocol was maintained while using 2,6-dimethylpyridine (about 580 μmol) and the data was collected after 6 h of continuous operation and the measured 2MP and the rates are reported in Table 5. The 2MP rate has drastically decreased after poisoning the catalyst surface particularly with 2,6-dimethylpyridine adsorption. A slightly higher rate of 2MP is found upon poisoning with pyridine compared to 2,6-dimethylpyridine. This could possibly be due to the persistence of Bronsted acid sites on the catalyst surface as pyridine is believed to be a Bronsted and Lewis acid site blocker.

4. Discussion

The 2MP rates have linearly decreased (Table 3) with increase in calcination temperature and correspondingly 2-pyrazinylmethanol rates are increased. The high temperature calcined Zn–Cr–O (ZC550, ZC650 and ZC750) samples showed lower number of surface hydroxy groups which displayed high rate of 2-pyrazinylmethanol probably because of decrease in acid-base strengths of Zn–Cr–O (Table 1). We believe that both acid-base sites strongly influence the further transformation of 2-pyrazinylmethanol, particularly basic sites (Bronsted or Lewis) on the Zn–Cr–O surface. Increased rates of 2-pyrazinylmethanol at high temperature calcined samples exemplifies that the homocoupling of 2-pyrazinylmethanol (Scheme 1) is curtailed probably due to decreased acid-base strengths of Zn–Cr–O sample.

The reduced Zn–Cr–O surface upon exposure to H_2O at 400 °C seems to convert the coordinatively unsaturated $M^{x+1}O^{2-}$ (M=Zn and/or Cr coordinatively unsaturated) species into HO^-–M^{x+}–$^-$OH hydroxy groups by dissociative adsorption [21]. These hydroxy groups possess Bronsted and Lewis acidity, although they behave as basic $^-$OH groups, because the bond with which they are coordinated to the metal cation is ionic. It was observed that the ZC450 sample demonstrated higher 2MP rates than the other Zn–Cr–O samples calcined above 450 °C. The TPD of CO_2 studies performed on the reduced catalysts revealed a specific CO_2 uptake ca. 25.2 μmol m^{-2} over ZC450; which is higher than the other ZC samples calcined at various temperatures (Table 1). It is anticipated that the hydroxy groups were generated on the catalyst surface during the course of reaction due to huge amounts of H_2O being passed along with glycerol and EDA. In the absence of H_2O in the reaction mixture (using pure glycerol and pure EDA) the ZC450 behaved as good as ZC650 sample (Table 3) (although EDA and glycerol conversions were low Table 4) as 2-pyrazinylmethanol selectivity was found to be 38.5%. The lower 2MP and higher 2-pyrazinylmethanol rates in the absence of H_2O may be explained due to scarcity of hydroxy groups that were reversibly generated in presence of H_2O. The ZC450 sample possessed moderate acidity [4] and slightly strong basic sites (25.2 μmol m^{-2}) that exhibited better 2MP yields than the other Zn–Cr–O samples.

It appears that reversible surface hydroxy groups are regenerated upon H_2O exposure to reduced Zn–Cr–O at 400 °C are more reactive than the one generated on unreduced Zn–Cr–O surface. To ascertain this; the best sample i.e. ZC450 has been subjected to three different treatments before measuring the CO_2 and NH_3

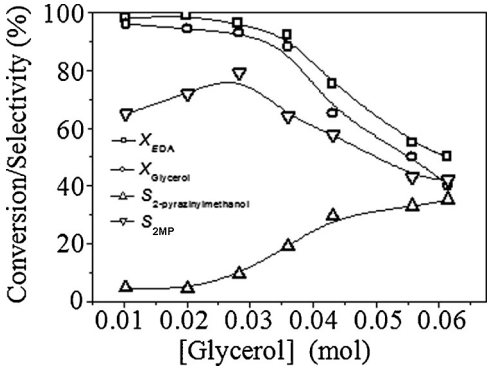

Fig. 13. Influence of glycerol loading on 2MP and 2-pyrazinylmethanol selectivities at a reaction temperature of 400 °C. Flow rate of reaction mixture = 5 mL h^{-1}; GHSV = 9.368 mL g_{cat}^{-1} s^{-1}.

Table 5
Influence of 2,6-dimethylpyridine and pyridine adsorption on 2MP rates over ZC450 sample.

Probe	[b]2,6-dimethylpyridine r_{2MP} (μmol s^{-1} m^{-2})	[c]Pyridine r_{2MP} (μmol s^{-1} m^{-2})
[a]Before	[a]25.8	[a]26.2
After	[b]3.5	[c]12.0

[a] ZC450 sample was reduced in 5%H_2/Ar at 400 °C/5 h prior to the reaction; flow rate of 5 mL h^{-1} (reaction mixture contained a glycerol:EDA:H_2O:N_2 = 1:1:20:8 mole ratio) at a reaction temperature of 350 °C.
[b] ZC450 sample was reduced in 5%H_2/Ar at 400 °C/5 h and a dose of 500 μmol of pyridine adsorbed at 350 °C followed by flushing the sample in N_2 at 350 °C/1 h prior to the reaction. The reaction mixture feed rate was 5 mL h^{-1} (reaction mixture contained a glycerol:EDA:H_2O:N_2 = 1:1:20:8 mole ratio) at a reaction temperature of 350 °C.
[c] ZC450 sample was reduced in 5%H_2/Ar at 400 °C/5 h and dose of 580 μmol of 2,6-dimethylpyridine adsorbed at 350 °C followed by flushing the sample in N_2 at 350 °C/1 h at a feed rate of 5 mL h^{-1} (reaction mixture contained a glycerol:EDA:H_2O:N_2 = 1:1:20:8 mole ratio.) and at a reaction temperature of 350 °C.

Table 6
The CO_2 and NH_3 uptakes of ZC450 (~0.1 g) sample measured by pulse chemisorption studies at 100 °C after oxidized, reduced and steam exposed conditions.

Probe	[a]Calcined in air	[b]Calcined in air followed by reduction	[c]Calcined in air followed by reduction and subsequent steam exposure
NH_3 uptake ($\mu mol\ g_{cat}^{-1}$)	65.5	96.4	64.2
CO_2 uptake ($\mu mol\ g_{cat}^{-1}$)	470.4	972.9	1537.5

[a] ZC450 sample degassed in He (30 mL min^{-1}) at 200 °C/5 h and the CO_2 uptake was measured by pulse chemisorption at 100 °C. After a similar treatment the NH_3 uptakes was measured by pulse chemisorption at 100 °C.

[b] ZC450 sample reduced at 400 °C/5 h in 5%H_2/Ar and the CO_2 uptake was measured at 100 °C. After a similar treatment the NH_3 uptakes was measured by pulse chemisorption at 100 °C.

[c] ZC450 sample reduced at 400 °C/5 h in 5%H_2/Ar followed by H_2O was exposed (with a dose of 0.2 mol) at 400 °C/1 h and then flushed at the same temperature in He (30 mL min^{-1}) for 1 h, subsequently the CO_2 uptake was measured at 100 °C. Under similar procedure the NH_3 uptakes was measured by pulse chemisorption at 100 °C. These experiments were carried out independently using about 0.1 g ZC450 sample with 10% NH_3 (balance helium) and/or 10.18% CO_2 balance helium.

uptakes by pulse chemisorption studies at 100 °C in a set of six independent experiments and the results are reported in Table 6.

Inspection of Table 6 revealed about 50% of acidity is increased after a reductive pretreatment when compared to the air calcined sample. The sample after successive treatments (reduction followed by steam exposure) showed equivalent amount of NH_3 uptake similar to the sample calcined in air. On the contrary the CO_2 uptakes were doubled after reduction and tripled with subsequent steam exposure. These results suggest that the ZC450 surface in reaction conditions; presence of large amount of H_2O (along with glycerol and EDA) seems to change the surface basicity enormously whereas the surface acidity was not much differed. These measurements clearly indicated that reduction of Zn–Cr–O enhanced both acid-base strength and the reduced surface with subsequent exposure to H_2O at 400 °C generated very strong basic sites and the acidic sites remains unchanged.

Baiker and co-workers reported that the reduced chromium oxide possess higher number of coordinatively unsaturated sites than the unreduced surface [28,29]. The intensity of the band due to surface hydroxy group (Fig. 3b) centred at 3428 cm^{-1} gradually decreased from 450 to 750 °C in the FT-IR spectra; probably because of condensation of adjacent hydroxy groups to form a network of M(II)–O–M(III) (metal–oxygen) bridged linkages at high temperatures [27]. As a result large size clusters of ZnO and $ZnCr_2O_4$ species were formed. This could be a reason why both H_2 and O_2 uptakes decreased with raise in calcination temperature of Zn–Cr–O samples. Elemental analysis of Zn–Cr–O sample calcined at various temperatures showed no leaching of either Zn or Cr.

The Cr^{6+} species were measured from the H_2 uptakes of Zn–Cr–O obtained with TPR analysis and the results are reported in Table 7 [30]. The Cr^{6+} concentration is decreased with increase in calcination temperature of the Zn–Cr–O sample. With increase in calcination temperature from 400 to 750 °C, Raman spectra of Zn–Cr–O (Fig. 5) revealed the decrease in band intensity at 996 cm^{-1}; the characteristic Cr=O stretching vibration due to Cr^{6+} species which is explained by self reduction of Cr^{6+} at high calcination temperatures in static air [31]. The partially reduction of chromium species is further evidenced from FT-IR, XPS, TPD of NH_3 and O_2 uptakes of Zn–Cr–O samples.

Table 7
Estimation of Cr^{6+} from H_2 uptakes obtained by TPR analysis of Zn–Cr–O sample calcined at various temperatures.

Sample	H_2 uptake ($\mu mol\ g_{cat}^{-1}$)	H_2 uptake ($\mu mol\ mg_{Cr}^{-1}$)	$\%Cr^{6+}$
ZC400	287.0	1.196	4.12
ZC450	104.3	0.443	1.52
ZC550	89.4	0.375	1.29
ZC650	62.1	0.255	0.88
ZC750	54.4	0.231	0.80

It was found that the rate of 2-pyrazinylmethanol was higher on high temperature calcined samples than the one calcined at low temperature. Existence of multiple oxidation states of chromium in Zn-spinel structure may be due to a polymeric network of Zn^{2+}–O–Cr^{3+} (in reduced form) and Zn^{2+}–O–Cr^{x+} ($3 \le x \le 6$) in unreduced state. This posed a pronounced difference in activity and selectivities during the dehydrocyclization reaction.

According to Sanderson's electro negativities of ions, the oxides of metals in higher oxidation state are also characterized by high covalency of M–O bond. The unsaturated metal cations are usually characterized by high Lewis acidity. The coordinatively unsaturated surface contains O^{2-} or ^{-}OH ions, which act as strong Lewis base. Evidence to this fact is obtained from the FT-IR spectra of Zn–Cr–O catalysts in which the intensity of hydroxy groups is strongly decreased at high calcination temperatures [32].

The FT-IR spectra of ZC450 fresh (calcined at 450 °C), reduced (air calcined followed by reduction in H_2 at 400 °C for 5 h), pyridine adsorbed (calcined in air followed by reduction and subsequent probe adsorption) and 2,6-dimethylpyridine (air calcined followed by reduction and subsequent probe adsorption) adsorbed are reported in Fig. 14. The bands appearing in the region 900 to 1120 cm^{-1} are evidences of Cr=O linkages present in the lattice. These Cr=O linkages represent the high valent state of chromium, possibly due to Cr^{6+} species as there is no evidence of any Cr^{5+} species, the other paramagnetic species in the ESR spectra.

The band intensity at 1116 cm^{-1} in fresh ZC450 sample (Fig. 14a) increased (Fig. 14b) upon reduction of ZC450 compared to fresh unreduced sample. An increase in band intensity at 1116 cm^{-1} (reduced sample) is accompanied by diminished band intensity at 911 cm^{-1} in unreduced catalyst (Fig. 14a and b). This change is probably due to increased coordinative unsaturation upon surface reduction. The band at 1624 cm^{-1} in fresh and reduced sample is shifted to 1578 cm^{-1} (Fig. 14c) a frequency difference by −46 cm^{-1} after pyridine adsorption. Similarly shift in frequency from 1624 to 1565 cm^{-1} (−59 cm^{-1}) is observed upon 2,6-dimethylpyridine adsorption (Fig. 14d). The vibrational perturbation due to polarization of lone pair electrons of adsorbate to adsorbent site caused the shift in band positions. Thus the changes/shift in band positions are attributed to adsorption of base probe molecules on acid sites present on the catalyst surface. The pronounced shift (−59 cm^{-1}) in vibrational frequencies indicates the strong interaction between surface acid site and 2,6-dimethylpyridine. In the comparative analysis the pyridine adsorption led to small shift than the 2,6-dimethylpyridine; may be because of adsorption of pyridine on both Lewis as well as on Bronsted acid sites simultaneously, as equimolar concentration of base probes were adsorbed on the catalyst surface.

The FT-IR spectra of pyridine adsorbed on Zn–Cr–O are consistent with the results reported by Guido Busca on pyridine adsorbed on $ZnCr_2O_4$ [21]. Pyridine coordinated on Lewis sites is characterized by bands appeared (Fig. 14c′) at 1454.2 and 1600–1637 cm^{-1} and the vibrational bands due to pyridinium ion (Bronsted acid sites) are characterized from the bands at 1553 and 1637.5 cm^{-1} are in good correlation with earlier reports [33,34]. FT-IR of 2,6-dimethylpyridine adsorbed (deconvoluted) spectra of Zn–Cr–O is reported in Fig. 14d′. Bands due to 2,6-dimethylpyridine coordinated to Lewis acid site is observed at 1449.3 cm^{-1}, whereas 2,6-dimethylpyridinium ion (Bronsted acid sites) is found at 1545.8 cm^{-1}. A shift in vibrational band to higher wavenumber in pyridine adsorbed spectra (1553 cm^{-1}) by a factor of 7.2 cm^{-1} when compared to 2,6-dimethylpyridine adsorbed (1545.8 cm cm^{-1}) on Bronsted acid sites is observed. A perturbed broad component near

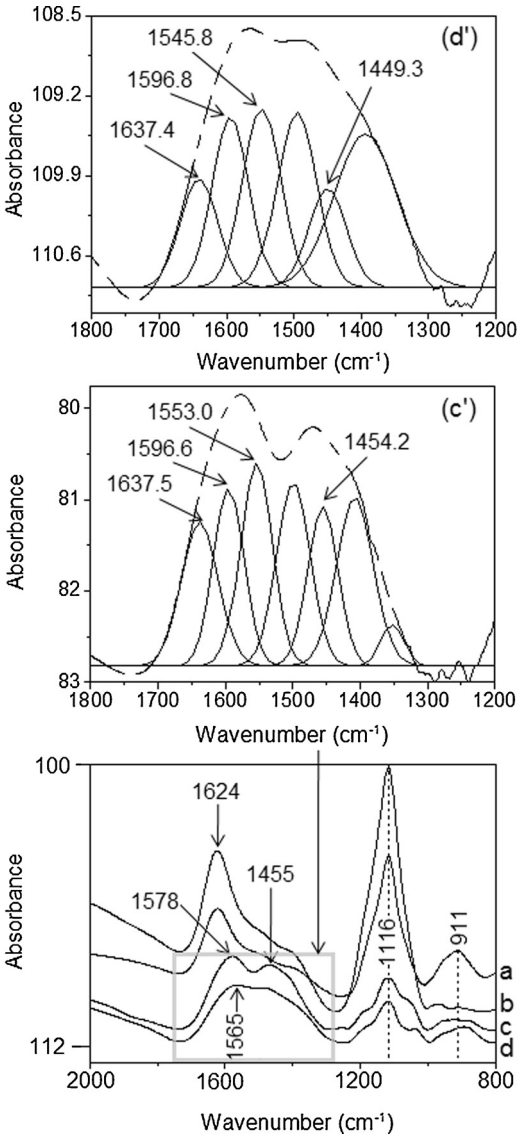

Fig. 14. FT-IR spectra of (a) fresh (calcined in air at 450 °C/5 h); (b) reduced (calcined in air at 450 °C/5 h followed by reductively pre-treated in 5%H_2/Ar at 400 °C/5 h); (c) pyridine adsorbed (calcined in air at 450 °C/5 h followed by reduction in 5%H_2/Ar at 400 °C/5 h and subsequently a dose of 500 μmol of pyridine (injected in 10 successive pulses in N_2 stream 30 mL min^{-1} on to catalyst at a temperature of 350 °C and flushed with N_2 at 350 °C/3 h); (d) 2,6-dimethylpyridine adsorbed (calcined in air at 450 °C/5 h followed by reduction in 5%H_2/Ar at 400 °C/5 h and subsequently a dose of 580 μmol of 2,6-dimethylpyridine (injected in 10 successive pulses in N_2 stream 30 mL min^{-1} on to catalyst at a temperature of 350 °C and flushed with N_2 at 350 °C/3 h) Zn–Cr–O samples measured in the range 800 to 400 cm^{-1}, and the (c′) the deconvoluted spectra of pyridine adsorbed Zn–Cr–O, and (d′) 2,6-deconvoluted spectra of 2,6-dimethylpyridine adsorbed Zn–Cr–O.

2314 cm^{-1} is noticed (SI) on 2,6-dimethylpyridine adsorbed surface, which is weak and may be due to H-bonding contributed from surface hydroxy groups [34].

The ratios of the normalized relative intensities of bands (Fig. 14c′ and d′) due to Lewis (around 1450 cm^{-1}) and Bronsted acid sites (1545 to 1553 cm^{-1}) are measured in order to compare the adsorption strength of pyridine and 2,6-dimethylpyridine. A ratio between $BA_{pyridine}$: $BA_{2,6\text{-dimethylpyridine}}$ = 1.0 and $LA_{pyridine}$: $LA_{2,6\text{-dimethylpyridine}}$ = 1.69 is observed. Thus suggests the pyridine adsorption is taking place on both Bronsted and Lewis acid sites in equal proportions whereas 2,6-diemethylpyridine adsorption is higher on Bronsted acid sites.

In case of ZnO–$ZnCr_2O_4$ mixed oxide; contribution of the surface acidity (mostly) whether Lewis or Bronsted is predicted by the presence of surface chromium not by ZnO. The ZnO particles with 19.8 nm in combination with $ZnCr_2O_4$ size of about 14.5 nm (Zn–Cr–O) showed higher 2MP yields than the other Zn–Cr–O samples those contained large crystallites of ZnO and $ZnCr_2O_4$.

Based on the product distribution and from the various kinetic studies it can be construed that the adsorption of glycerol seems to take place on Zn particles than on chromium species as the individual bulk oxides showed enormous differences on 2MP yields (Table 2). ZnO surface favored cyclization of glycerol with EDA whereas Cr_2O_3 seems to prefer inter molecular cyclization of EDA. Bulk $ZnCr_2O_4$ demonstrated better 2MP selectivity although the conversions were little lower than ZnO. Rate of 2MP is higher over a combination of ZnO–$ZnCr_2O_4$ surface than the bulk oxides and is in the order of Zn–Cr–O > $ZnCr_2O_4$ > ZnO > Cr_2O_3. It is noteworthy to mention that bulk ZnO produced about 9.8 μmol s^{-1} m^{-2} of 2-pyrazinylmethanol which was reduced to half ~4.8 μmol s^{-1} m^{-2} in case of $ZnCr_2O_4$ sample. Presence of ZnO species in the vicinity of $ZnCr_2O_4$ particles appears to activate glycerol and EDA to undergo cyclocondensation to form 2-pyrazinylmethanol and chromium species in the ZnO matrix seems to promote the homo-coupling of 2-pyrazinylmethanol which subsequently transformed to 2-pyrazinealdehyde and 2MP as noticed that the bulk ZnO and Cr_2O_3 were inferior in 2MP rates than the bulk $ZnCr_2O_4$. Interestingly all the samples (ZC400 to ZC750) showed very low amount of 2-pyrazinaldehyde compared to 2-pyrazinylmethanol (Scheme 1). Hence hydrogenation of 2-pyrazinaldehyde did not suffer much when compared to homo-coupling of 2-pyrazinylmethanol on the high temperature calcined Zn–Cr–O samples. From the activity data it appears that surface hydroxy groups are involved in the homo-coupling of 2-pyrazinylmethanol. Lack of sufficient number of surface hydroxy groups over high temperature calcined samples may be the reason for the lower 2MP and higher 2-pyrazinylmethanol rates. The reason for lower 2MP rate on ZC400 is attributed to strong acid and moderate basic sites present on the catalyst (Table 1) and another reason may be due to the absence of crystalline ZnO and $ZnCr_2O_4$ species (Fig. 1). The Zn–Cr–O sample (e.g. ZC450) possessed moderate acidity with strong basicity were active for both cyclocondensation of glycerol and EDA in the first step followed by homo-coupling of 2-pyrazinylmethanol to produce 2MP. In contrast homo-coupling of 2-pyrazinylmethanol is curtailed over Zn–Cr–O probably because of weak acidic and weak basic sites (e.g. ZC750).

5. Conclusions

XRD spectra of Zn–Cr–O showed resolved diffraction lines due to ZnO and $ZnCr_2O_4$ phases attributed to large size crystallite formation at high temperature calcination. TPR analysis revealed the decreased H_2 uptakes on high temperature calcined Zn–Cr–O. Disappearance of the bands typical for the vibrations of CrO_4 tetrahedra at 933–928 and 952 cm^{-1} due to reduction of $Cr^{6+} \rightarrow Cr^{3+}$ may be a reason for the decreased H_2 uptakes. It was further evidenced due to a shift in Cr2p binding energy from 578.1 (Cr^{6+}) to 576.3 eV (Cr^{3+}) from ZC400 to ZC750 samples. The characteristic Cr=O (Cr^{6+}) stretching vibration of Raman band around ~996 cm^{-1} was decreased at high calcination temperatures further indicated the reduction of Cr^{6+} species. Reduction of Cr^{6+} to Cr^{3+} species at high temperature calcination was examined O_2 pulse chemisorption studies that showed lower O_2 uptakes on high temperature calcined samples. The Zn–Cr hydrotalcite precursor at low calcination temperatures generated mixed oxides of ZnO–$ZnCr_2O_4$ was found to be active and selective for dehydrocyclization of glycerol and EDA for 2MP synthesis. The unreduced

Zn–Cr–O catalyst produced higher pyrazine and reduced Zn–Cr–O demonstrated excellent 2MP yields. A reductive pretreatment is necessary for ZnO–$ZnCr_2O_4$ catalyst in order to obtain higher 2MP yields. 2MP selectivity was found to be dependent on acid-base strength and crystallite size of Zn–Cr–O catalysts. Physicochemical characteristics of the mixed oxides revealed that low temperature treated Zn–Cr–O produced 2MP in good to excellent yields and the high temperature treatment produced 2-pyrazinylmethanol in large quantities. Crystallite size and O_2 uptakes of Zn–Cr–O emphasized that small size ZnO–$ZnCr_2O_4$ mixed oxides are suitable for better selectivity of 2MP whereas large sized Zn–Cr–O delivered 2-pyrazinylmethanol. Rate of 2-pyrazinylmethanol was increased with increasing calcination temperature which is attributed to decrease in the surface hydroxy groups on the Zn–Cr–O surface. Decrease in NH_3 uptakes are clearly observed in TPD of NH_3 studies. The ZC450 sample with a CO_2 uptake of 25.2 $\mu mol\, m^{-2}$ was 2MP selective. The catalytic activity studies under surface poisoning conditions exemplified that 2MP rate was better after pyridine adsorption compared to 2,6-dimethylpyridine. Acidity of Zn–Cr–O was remaining unchanged when subjected to calcination–reduction-steam exposure; contrarily basicity was tripled with the sequential treatments. From the catalyst poisoning studies it can be concluded that a combination of acid-base pair is desirable for 2MP. Particularly a pair of weak acid and strong base sites may be active for dehydrocyclization of EDA and aqueous glycerol for 2MP synthesis.

Acknowledgments

One of the authors RS, VK, CA thank CSIR New Delhi for the award of JRF; MKK thank UGC New Delhi for JRF and AV thank Dr M Lakshmi Kantam and Dr K S Rama Rao for their constant help and encouragement. Financial support from CSIR New Delhi under INDUS-MAGIC program CSC-0123 is acknowledged.

Appendix A. Supplementary data

Supplementary data associated with this article can be found, in the online version, at http://dx.doi.org/10.1016/j.apcata.2013.10.023.

References

[1] C.-H. (Clayton) Zhou, J.N. Beltramini, Y.-X. Fan, G.Q. (Max) Lu, Chemical Society Reviews 37 (2008) 527–549.
[2] R. Sarkari, Ch. Anjaneyulu, V. Krishna, R. Kishore, M. Sudhakar, A. Venugopal, Catalysis Communications 12 (2011) 1067–1070.
[3] L. Forni, Journal of Catalysis 111 (1988) 199–209.
[4] A. Venugopal, R. Sarkari, Ch. Anjaneyulu, V. Krishna, M. Kotesh Kumar, Applied Catalysis A: General 441–442 (2012) 108–118.
[5] E.V. Ramos-Fernández, A.F.P. Ferreira, A. Sepúlveda-Escribano, F. Kapteijn, F. Rodríguez-Reinoso, Journal of Catalysis 258 (2008) 52–60.
[6] E.L. Crepaldi, P.C. Pavan, W. Jones, J.B. Valim, Studies in Surface Science and Catalysis 129 (2000) 691–700.
[7] M. Ohta, Y. Ikeda, A. Igarashi, Applied Catalysis A: General 258 (2004) 153–158.
[8] R.B. Fahim, M.I. Zaki, A.M. El-Roudi, A.M.A. Hassaan, Journal of the Research Institute for Catalysis 29 (1) (1981) 25–36.
[9] B. Grzybowska, J. Sloczynski, R. Grabowski, K. Wcislo, A. Kozlowska, J. Stoch, J. Zielinski, Journal of Catalysis 178 (1998) 687–700.
[10] G.N. Pirogova, N.M. Panich, R.I. Korosteleva, Yu.V. Voronin, N.N. Popova, Russian Chemical Bulletin International Edition 50 (12) (2001) 2377–2380.
[11] G.V. Itina, A.A. Davydov, M.A. Osipova, L.N. Kurina, Reaction Kinetics and Catalysis Letters 45 (2) (1991) 243–249.
[12] M. Galeotti, M. Torrini, U. Bardi, A. Santucci, D. Ghisletti, Surface Science 375 (1997) 63–70.
[13] Z.V. Marinkovic, L. Mancic, P. Vulic, O. Milosevic, Journal of European Ceramic Society 25 (2005) 2081–2084.
[14] E.F. Kozhevnikov, I.V. Kozhevnikov, Journal of Catalysis 238 (2006) 286–292.
[15] F. Cavani, M. Koutyrev, F. Trifiro, A. Bartolini, D. Ghisletti, R. Iezzi, A. Santucci, G.D. Piero, Journal of Catalysis 158 (1996) 236–250.
[16] Z.V.M. Stanojević, N. Romčević, B. Stojanović, Journal of European Ceramic Society 27 (2007) 903–907.
[17] M.A. Vuurman, F.D. Hardcastle, I.E. Wachs, Journal of Molecular Catalysis 84 (1993) 193–205.
[18] B.M. Weckhuysen, I.E. Wachs, Journal of Physical Chemistry 100 (1996) 14437–14442.
[19] L. Forni, P. Pollesel, Journal of Catalysis 130 (1991) 403–410.
[20] B.M. Latha, V. Sadasivam, B. Sivasankar, Catalysis Communications 8 (2007) 1070–1073.
[21] G. Busca, Catalysis Today 41 (1998) 191–206.
[22] C. Liu, C. Xu, T. Xia, Y. Guo, J. Liu, Heteroatom Chemistry 23 (4) (2012) 377–382.
[23] I.M. Goldman, Journal of Organic Chemistry 27 (7) (1963) 1921–1923.
[24] H. Rutner, P.E. Spoerri, Journal of Organic Chemistry 28 (7) (1963) 1898–1899.
[25] Y. Houminer, Journal of Organic Chemistry 45 (6) (1980) 999–1003.
[26] M.A. Dasari, P. Kiatsimkul, W.R. Sutterlin, G.J. Suppes, Applied Catalysis A: General 281 (2005) 225–231.
[27] E.P. Parry, Journal of Catalysis 2 (1963) 371–379.
[28] H.E. Curry-Hyde, H. Musch, A. Baiker, M. Schraml-Marth, A. Wokaun, Journal of Catalysis 133 (1992) 397–414.
[29] M. Schraml-Marth, A. Wokaun, H.E. Curry-Hyde, A. Baiker, Journal of Catalysis 133 (1992) 431–444.
[30] A.B. Gaspar, J.L.F. Brito, L.C. Dieguez, Journal of Molecular Catalysis A: Chemical 203 (2003) 251–266.
[31] P. Wilson, P. Madhusudhan Rao, R.P. Viswanath, Thermochimica Acta 399 (2003) 109–120.
[32] M. Takeuchi, L. Bertinetti, G. Martra, S. Coluccia, M. Anpo, Applied Catalysis A: General 307 (2006) 13–20.
[33] C.U.I. Odenbrand, J.G.M. Brandin, G. Busca, Journal of Catalysis 135 (1992) 505–517.
[34] A. Travert, A. Vimont, A. Sahibed-Dine, M. Daturi, J.-C. Lavalley, Applied Catalysis A: General 307 (2006) 98–107.